Predicting deghosted reflection data for both pressure and multicomponent displacements at the ocean bottom

Jing Wu and Arthur B. Weglein, M-OSRP, University of Houston

SUMMARY

Deghosting is a key step for ocean bottom seismic data processing. For measurements at the seafloor, notches can occur within the spectrum at much lower frequencies than for towed streamer data. Removing ghosts can improve seismic resolution. In addition, the subsequent steps (e.g., multiple removal, imaging and inversion) will all benefit from effective deghosting. In this paper, based on Green's theorem, we provide distinct methods to separate (1) the pressure data that are collected just above ocean bottom, and (2) the multicomponent displacements that are acquired below the seafloor, into up and down waves. Synthetic tests demonstrate the promise and potential of this method for deghosting ocean bottom data.

INTRODUCTION

Ocean bottom acquisition is used in offshore exploration to improve the S/N, providing a quieter seafloor environment compared to conventional streamer data acquisition. However, ghosts are more serious for ocean bottom measurements. Here is a simple example to illustrate the significance and issue (Weglein et al., 2013). The frequency of the first notch can be approximately $f = c/(2z)$ at near offset, where c is water speed, and z is the depth of streamer. For typical towed streamer data at 6 m, a receiver notch occurs at 125 Hz, which is usually outside data spectrum; however, for ocean bottom data at 150 m, the first notch can come in at 5 Hz. This example indicates that ghost is a serious problem for ocean bottom data, since the notches are inside the seismic bandwidth. Therefore, deghosting the reflection data is an essential step in ocean bottom data analysis. In addition, this wave separation step is an important prerequisite for inverse scattering algorithms to remove free surface and internal multiples. One step further, it is also required to enhance structural analysis and amplitude analysis.

Among the wave separation methods, the distinct advantages of Green's theorem wave separation method have been demonstrated and discussed in order to separate the reference and scattered waves, and to deghost for offshore plays (Weglein and Secrest, 1990; Weglein et al., 2002; Zhang, 2007; Mayhan and Weglein, 2013; Tang et al., 2013). The continued work by Wu and Weglein (2014, 2015a,b) extended this method for land data to deal with ground roll issues. Inherently, the Green's theorem based wave-separation method starts with a reference medium for the interest of a certain purpose and characterizes the difference between actual world and reference medium as sources. Within wave-separation task, different applications call for different choices of reference media. For example, based on the same general wave-separation idea from Green's theorem, the pressure data deghosting employs a whole space of water as reference (Zhang and Weglein, 2006), while the displacement data deghosting adopts a whole space of elastic medium.

In this paper, we apply the Green's theorem based wave separation algorithms for both pressure and displacements at ocean bottom. This application requires multicomponent data and no assumption or limitation of acquisition topography. Synthetic data examples are presented to show the effectiveness of the methods for deghosting pressure and displacement data respectively.

OCEAN BOTTOM DATA ACQUISITION AND BOUNDARY CONDITIONS

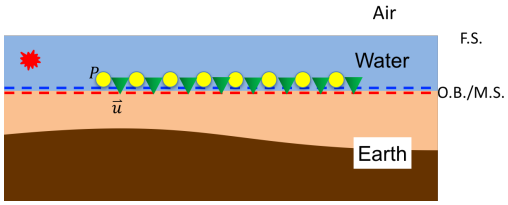

Figure 1: Acquisition at ocean bottom; the yellow circles represent hydrophones; and the green triangles are for geophones. The conventions used in this paper: F. S. for free surface, or air/water boundary for preciseness; M. S. for measurement surface; O. B. for ocean bottom.

As is shown in Figure 1, a generic ocean bottom experiment is applied on a model consisting of an air half-space, and a water layer, and then the heterogeneous earth. An airgun is located in the water. We put hydrophones just above the ocean bottom to measure the pressure (P) of water. And we put geophones slightly below ocean bottom to measure multicomponent wave displacements ($\vec{u}$) of earth. The displacements contain both longitudinal waves and share waves, which agree with the actual ocean bottom measurements.

On either side of the ocean bottom, traction is continuous along both normal direction and tangential direction, and displacement is continuous along normal direction. Hence,

$$u_{\mathbf{wn}} = \vec{u} \cdot \hat{n}, \tag{1}$$

where $u_{\mathbf{wn}}$ is the displacement in the water along the normal direction at ocean bottom, $\vec{u}$ is the measured multicomponent displacements of earth, and $\hat{n}$ is the normal vector towards the lower side.

Besides,

$$\vec{t_{\mathbf{e}}} = -P\hat{n}, \tag{2}$$

where $\vec{t_{\mathbf{e}}}$ is traction at ocean bottom in the earth, and P is the measured pressure of water. The traction is zero along the tangential direction.

PRESSURE WAVE SEPARATION THEORY

We choose the reference medium as a homogenous acoustic whole space water (Figure 2), having the same properties with the reality along the measurement surface. There are three sources (Figure 3) acting on the selected reference medium, which are energy source (S_1), air perturbation S_2, and earth perturbation S_3, respectively. S_1 produces the direct wave, a type of downgoing waves; S_2 transfers all the upgoing waves into down waves, so called ghosts at receiver side; S_3 generates up waves from the earth, including the upward reflections from both the ocean bottom and earth beneath ocean bottom. Choosing a closed semi-infinite surface bounded below by the measurement surface (Figure 3), and evaluating the surface integration inside the volume, then the portion of the wavefield due to the source outside the volume can be produced; i.e., the contribution of S_3, which is upgoing wave, can be predicted inside the volume.

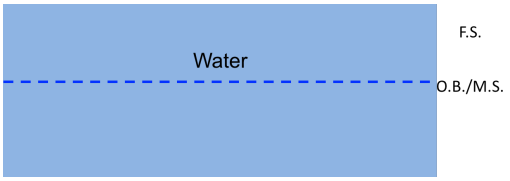

Figure 2: A homogeneous whole-space acoustic reference medium for deghosting the pressure data.

With Equation 1 and the relationship below

$$\rho\omega^2 u_{\mathbf{wn}} = \frac{\partial P}{\partial n}, \tag{3}$$

where ρ is water's density, the pressure wave separation formula based on the Green's theorem is

$$\begin{aligned} & P^{up}(\vec{r},\omega) \\ &= \int_{m.s.} [P(\vec{r}',\omega)\nabla' G_0(\vec{r}',\vec{r},\omega) - G_0(\vec{r}',\vec{r},\omega)\nabla' P(\vec{r}',\omega)] \cdot \hat{n} d\vec{r}' \\ &= \int_{m.s.} [P(\vec{r}',\omega)\frac{\partial G_0(\vec{r}',\vec{r},\omega)}{\partial n} - \rho\omega^2 G_0(\vec{r}',\vec{r},\omega) u_{\mathbf{wn}}(\vec{r}',\omega)] d\vec{r}', \end{aligned} \tag{4}$$

where G_0 is the scalar Green's function in the reference medium of water; P^{up} is the predicted upgoing wave.

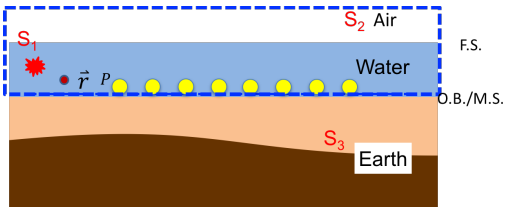

Figure 3: The integral provides the contributions from S_3, for evaluation point $\vec{r}$ inside the volume.

DISPLACEMENT WAVE SEPARATION THEORY

The displacements represent the motion of earth close to water / elastic-earth boundary. It is similar to land acquisition in the way that receivers are close to acoustic / elastic-earth boundary and collecting particles' vibration of the earth. Therefore, the ghost removal algorithm for land displacement data can be extended to ocean bottom.

The reference medium is selected as a homogenous elastic whole space, whose property agrees with the actual earth along the measurement surface. There are four sources. Among them, the energy source S_1, air perturbation S_2, and water perturbation S_3 are above the measurement surface and, collaborate to produce the direct waves and ghosts, which are downgoing waves. At receiver side, the ghosts can have their last downward reflections at either air/water boundary or water/earth boundary. On the other side, the earth perturbation S_4 generates upgoing reflections. Similar to the theory for deghosting pressure data, Green's theorem based surface integration along the measurement surface can predict the wavefield inside the enclosed volume but caused by S_4, which is the only upgoing portion of wavefield, also called the receiver-side deghosted wave field.

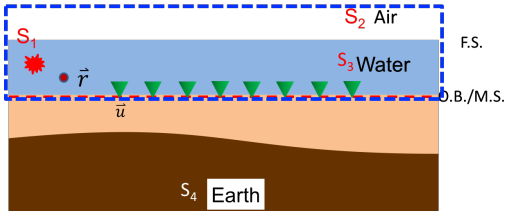

Figure 4: The integral extracts the contributions from S_4, for evaluation point $\vec{r}$ inside the volume.

Using Equation 2, the Green's theorem wave separation formula for displacement data is

$$\begin{aligned} & \vec{u}^{up}(\vec{r},\omega) \\ &= -\int_{m.s.} [\vec{t}_{\mathbf{e}}(\vec{r}',\omega)\cdot\mathbf{G}_0(\vec{r}',\vec{r},\omega) - \vec{u}(\vec{r}',\omega)\cdot(\hat{n}\cdot\Sigma_0(\vec{r}',\vec{r},\omega))] d\vec{r}' \\ &= \int_{m.s.} [P(\vec{r}',\omega)\hat{n}\cdot\mathbf{G}_0(\vec{r}',\vec{r},\omega) + \vec{u}(\vec{r}',\omega)\cdot(\hat{n}\cdot\Sigma_0(\vec{r}',\vec{r},\omega))] d\vec{r}', \end{aligned} \tag{5}$$

where $\mathbf{G}_0$ is the Green's displacement tensor, Σ_0 is the Green's stress tensor; and $\vec{u}^{up}$ is the predicted upgoing wave.

There are three important points with respect to Equation 4 and 5: (1) No source information is required, neither amplitude nor radiation pattern. (2) The integrals are carried out at receiver side only and work on one experiment at a time, resulting in relatively small data requirement and low computational cost. (3) There is no assumption about the shape of the measurement surface – it can be flat, inclined, or undulating; i.e., the formulas can accommodate any topography of the ocean bottom.

NUMERICAL EVALUATION

In this section, we conduct a 2D line source experiment as an example to illustrate the performance of Green's theorem in separation of pressure just above the ocean bottom, and separation of displacements just below the ocean bottom into their

upgoing and downgoing portions respectively. The model is shown in Figure 5, and the parameters are listed in Table 1. The output point $\vec{r}$ is on the measurement surface but arranged to be part of the volume above by applying the wave separation formula in (k_x, ω) domain (see, e.g., Weglein et al. (2013)).

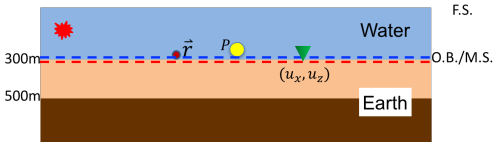

Figure 5: Synthetic model for numerical test.

Layer's Number	P Velocity (m/s)	S Velocity (m/s)	Density (kg/m^3)
1	1500	0	1000
2	2500	1200	2000
3	4000	1400	2000

Table 1: The parameters of the model in Figure 5.

Pressure wave separation

The wave separation results of pressure data are shown in Figure 8. By subtracting the predicted upward waves (Figure 8 (b)) from the total waves (Figure 8 (a)), we obtain the downward waves (Figure 8 (c)). Several early-arriving events (depicted with yellow arrows) of upgoing and downgoing waves are selected to plot the ray paths to understand their meanings. The ray plots are illustrated in Figure 6, where the measurement surface is plotted slightly above the ocean bottom for the convenience of comparison; however, the measurement surface is actually right sitting on the ocean bottom. Therefore, there are up-wave-down-wave pairs, such as $U1/D1$, $UM1/DM1$ and $UM2/DM2$, which have the same arriving times. There is no corresponding downgoing wave to the upgoing wave $U2$, the primary from the second reflector; hence at the time zone of $U2$, the downgoing wave in Figure 8(c) is blank. Even the pressure waves are measured at the end, which could have shear wave history at the second layer; e.g., $U2$, $UM2$, and $DM2$ consist of three events, with $\grave{P}\acute{P}$, $\grave{P}\acute{S}/\grave{S}\acute{P}$, and $\grave{S}\acute{S}$ at the bottom of the second layer.

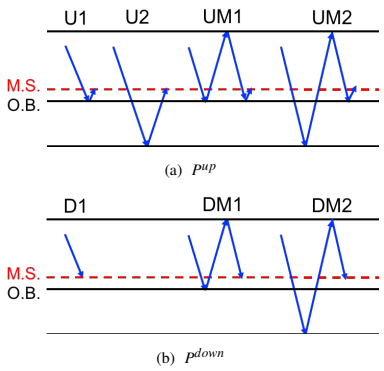

Figure 6: The ray path plots of depicted events in Figure 8. (a) for up waves; (b) for down waves.

Displacement wave separation

The wave separation results of multicomponent displacements are shown in Figure 9 for x component and Figure 10 for z component. The down waves are obtained by subtracting the separated upgoing waves from the total wavefields. To further understand the results, the z component results are selected to analyze the ray path of early-arriving events (depicted with yellow arrows). The ray plots are shown in Figure 7, where the measurement surface is put slightly below the ocean bottom so that we can see clearly the downgoing waves whose last reflections happen at the ocean bottom; however, the measurement surface is actually right beneath the ocean bottom. Similarly, the up-wave-down-wave pairs, such as $U2/D2$, and $UM2/DM2$, arrive simultaneously. The downgoing waves, all the propagation is within the water layer, have no companion up waves; thereby, at the time zones of $D1$, $DM1$, and $DM11$, the upgoing wave plot in Figure 10(b) is blank. Besides, there are internal multiples in the shot records and two events are pointed out by the red arrows in Figure 10(b).

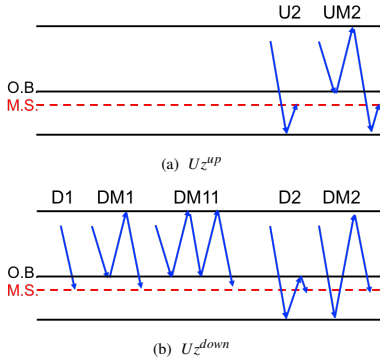

Figure 7: The ray path plots of depicted events in Figure 10. (a) for up waves; (b) for down waves.

CONCLUSION

By choosing appropriate reference media, the Green's theorem wave separation concepts can be extended and applied to ocean bottom data. This method can effectively separate the pressure, and the multicomponent displacements, into their up and down parts. In this paper, we provide a general wave separation formula which has three advantages: (1) it doesn't require source information; (2) it works on one experiment at a time, and has low computation cost; (3) it can accommodate the measurement surface without any topographic assumption or limitation, and is well suited for complicated ocean bottom problems. The synthetic example in this paper using a horizontal layered model indicates that the algorithm works yielding positive and encouraging results.

ACKNOWLEDGEMENTS

We are grateful to all M-OSRP sponsors for encouragement and support in this research.

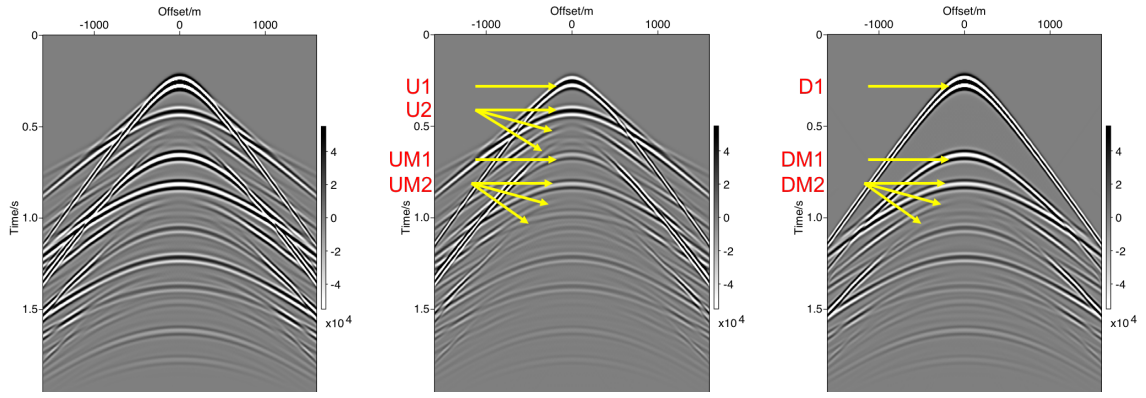

(a) P (b) P^{up} (c) P^{down}

Figure 8: Wave separation on pressure field. (a) for total wave; (b) for up wave; (c) for down wave.

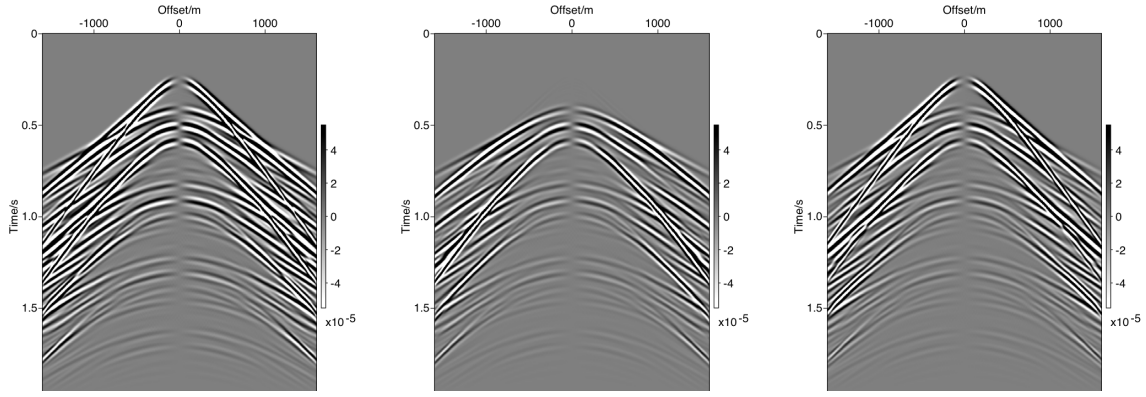

(a) Ux (b) Ux^{up} (c) Ux^{down}

Figure 9: Wave separation on x component of displacement field. (a) for total wave; (b) for up wave; (c) for down wave.

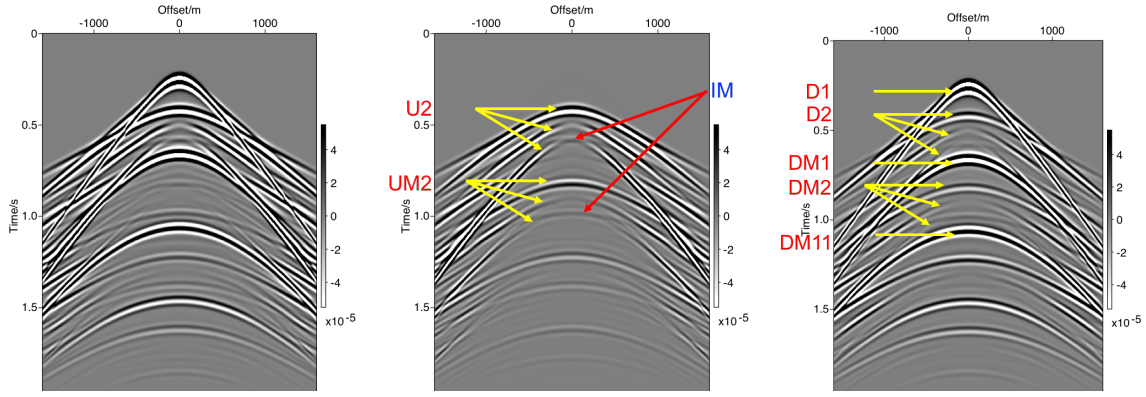

(a) Uz (b) Uz^{up} (c) Uz^{down}

Figure 10: Wave separation on z component of displacement field. (a) for total wave; (b) for up wave; (c) for down wave.

REFERENCES

Mayhan, J. D., and A. B. Weglein, 2013, First application of Green's theorem-derived source and receiver deghosting on deep-water Gulf of Mexico synthetic (SEAM) and field data: Geophysics, **78**, WA77–WA89.

Tang, L., J. D. Mayhan, J. Yang, and A. B. Weglein, 2013, Using Green's theorem to satisfy data requirements of multiple removal methods: The impact of acquisition design: 83rd Annual International Meeting, SEG, Expanded Abstracts, 4392–4396.

Weglein, A. B., J. Mayhan, L. Amundsen, H. Liang, J. Wu, L. Tang, Y. Luo, and Q. Fu, 2013, Green's theorem deghosting algorithms in (k,ω) as a special case of (x,ω) algorithms.: Journal of seismic exploration, **22**, 389–412.

Weglein, A. B., and B. G. Secrest, 1990, Wavelet estimation for a multidimensional acoustic earth model: Geophysics, **55**, 902–913.

Weglein, A. B., S. A. Shaw, K. H. Matson, J. L. Sheiman, R. H. Solt, T. H. Tan, A. Osen, G. P. Correa, K. A. Innanen, Z. Guo, and J. Zhang, 2002, New approaches to deghosting towed-streamer and ocean-bottom pressure measurements: 72th Annual International Meeting, SEG, Expanded Abstracts, 1016–1019.

Wu, J., and A. B. Weglein, 2014, Elastic Green's theorem preprocessing for on-shore internal multiple attenuation: theory and initial synthetic data tests: 84th Annual International Meeting, SEG, Expanded Abstracts, 4299–4304.

———, 2015a, Preprocessing in displacement space for on-shore seismic processing: removing ground roll and ghosts without damaging the reflection data: 85th Annual International Meeting, SEG, Expanded Abstracts, 4626–4630.

———, 2015b, Preprocessing in PS space for on-shore seismic processing: removing ground roll and ghosts without damaging the reflection data: 85th Annual International Meeting, SEG, Expanded Abstracts, 4740–4744.

Zhang, J., 2007, Wave theory based data preparation for inverse scattering multiple removal, depth imaging and parameter estimation: analysis and numerical tests of Green's theorem deghosting theory: PhD thesis, University of Houston.

Zhang, J., and A. B. Weglein, 2006, Application of extinction theorem deghosting method on ocean bottom data: 76th Annual International Meeting, SEG, Expanded Abstracts, 2674–2678a.